OBSERVATIONS OF PRECIPITATION DEVELOPMENT – AN EXAMPLE FROM THE UAE PROJECT

Daniel Breed, Tara Jensen, and Roelof Bruintjes
National Center for Atmospheric Research
Boulder, CO 80307

Abstract. Radar and aircraft observations from the 12 September 2004 case study, collected during a field project in the United Arab Emirates, are presented in the context of discerning precipitation development. The focus of the field projects was convective clouds forming over and near the Oman mountains in the eastern Arabian Penisula, as part of a larger feasibility study on precipitation enhancement and a subsequent randomized cloud seeding experiment. The radar data show that earlier convection likely pre-conditioned the region with mid-level moisture and ice particles. Subsequent cells and storms developed significant precipitation as they grew above 6 km (around -5° C). This is consistent with the concept that recycling particles into the same and adjacent turrets is an important process in precipitation development. However, the data set presented is quite limited and more details from other cases (both seeded and unseeded) are needed to generalize precipitation development in UAE clouds.

1. INTRODUCTION

Understanding precipitation development is key to several long standing problems in the atmospheric sciences, including precipitation forecasting and cloud seeding for precipitation enhancement. One of the tools for discerning precipitation processes has been and continues to be the meteorological radar. Implementation of new technology has expanded the capabilities of radar – for example, faster and less expensive hardware have allowed for more specialized radars operating over a broad range of wavelengths and yielding polarimetric information. However, most field projects in weather modification rely on reflectivity measurements from X-, C-, or S-band radar, which are still capable of providing limited information on precipitation development.

Studies of the first echo from radar (height, growth rate, etc.) have been able to discern warm rain processes and ice phase processes in a number of regions (e.g., Knight *et al.,* 1983; Dye *et al.,* 1983; Prakash, 1998). However, ambiguities can still exist even with survey or statistical types of studies. More detailed approaches have utilized cloud-penetrating aircraft, trajectory analyses, or numerical models to better understand precipitation formation, often in relation to other processes such as cloud seeding or electrification (e.g., Raymond and Blyth, 1989; Huston, *et al.,* 1991; Willis *et al.,* 1994; and others). The difficulties in understanding precipitation development in a broad sense for a particular area stem from the inadequacies of generalizing from case studies or the ambiguities inherent in statistical studies using coarse data.

Multiple paths exist for trying to address these difficulties, and our work in the United Arab Emirates (UAE) is attempting to follow a couple different approaches to discern precipitation development. This paper outlines a brief sample of the type of data being analyzed as an introduction to the overall aspects of the UAE project.

2. BACKGROUND

Over the last four years, a number of field projects have been conducted in the UAE as part of a feasibility study to assess the potential for rainfall enhancement via cloud seeding. Different aspects were addressed including trace gas and aerosol characterizations, hygroscopic flare development, radar reflectivity measurements, hydrological studies, cloud seeding trials, numerical model simulations, and collection of cloud microphysical data.

During the summer, the studies have concentrated on investigating convective clouds forming over the Al Hajir Mountains, known more generally as the Oman Mountains, along and east of the border between the UAE and Oman in the eastern region of the Arabian Penisula. Climatologically, January through March is the peak rainfall period in the UAE (although most recording stations are well away from the mountains), which is caused by the occasional westerly trough and frontal system passing through the region and providing extended periods of rainfall. However, summertime convection contributes a significant (and less variable) portion of the total annual precipitation in the eastern Arabian Peninsula.

The characteristics of summer convective storms resemble those of air mass storms in many other regions. The majority are relatively short-lived, although long-lived multi-cellular systems exist that produce a large fraction of the total precipitation from summer storms. Figure 1 shows a plot of the duration of storms from the summers of 2001 and 2002 as defined by a 30 dBZ threshold (via the TITAN software as described by Dixon and Weiner, 1993). The data are from the Al Dhafra radar, which: 1) was not consistently calibrated through the data collection period; 2) was west of the mountain convection by 120 km or more; and 3) was only completing a volume scan every 10 min. Because of the relatively poor temporal and spatial resolution of the data, the TITAN analysis has limitations. Nonetheless, more detailed data taken in 2003 and 2004 show similar trends in storm duration.

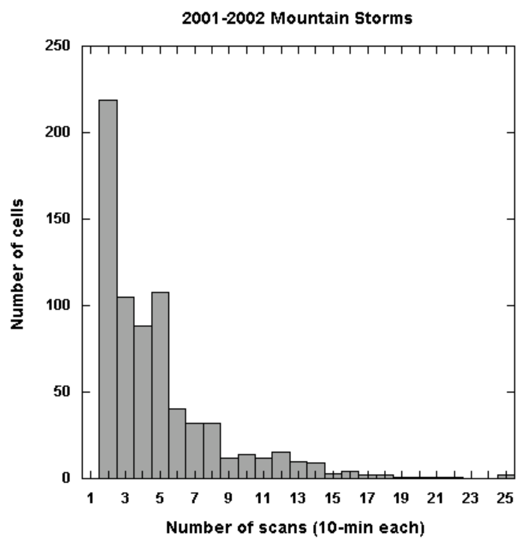

Figure 1. Histogram of cell duration (in number of volume scans) for 715 storms over the Oman mountains in 2001 and 2002. One volume is 10 min (i.e., 6 equals 1 hr).

During the summers of 2003 and 2004, a randomized seeding experiment was conducted using hygroscopic flares ignited in updrafts at cloud base. A major component of this experiment included making airborne microphysical measurements designed to elucidate the development of precipitation in order to verify steps in the conceptual seeding model. Some of those steps involve drizzle formation and recirculation or dispersion throughout the treated cell or turret and into neighboring turrets. The role of drizzle and larger drops in the graupel formation and riming processes is also viewed as integral to precipitation development (and enhancement) in these storms.

While conceptually straightforward, the microphysical details of individual cases are not usually as clear and multiple cases are needed to generalize the results. Several cases from the summers of 2003 and 2004 are being synthesized to examine the validity of the conceptual model, and one of them from 12 September 2004 is described in some detail here. The radar data are from a C-band radar, located at Al Ain airport about 40-80 km from the storms described below. Volume scans of 11 elevation angles were completed every 5 min, and the data were reduced in realtime onto a 750 m grid. Microphysical data were collected using the South African Aerocommander aircraft with a suite of PMS probes as well as the usual sensors measuring state parameters.

3. INITIAL STORM CHARACTERISTICS

Data from 12 September 2004 are the focus of this paper but data from a convectively active day, 10 July 2004, are also presented for comparison. A 12Z sounding from Abu Dhabi, taken about 120 km west of the area of interest, is plotted for each day in Figures 2 and 3. (The sounding data are from http://weather.uwyo.edu/upperair/sounding.html). They show typical characteristics of the thermodynamic structure in which summer storms develop. Most prominent is the dry, stable layer beginning at 500-550 hPa. The strength of this layer (or lack thereof), caused by large scale subsidence, often determines the formation of storms and their strength. Low-level moisture and mesoscale circulations over the mountains, not represented in the Abu Dhabi sounding, are other major determinants.

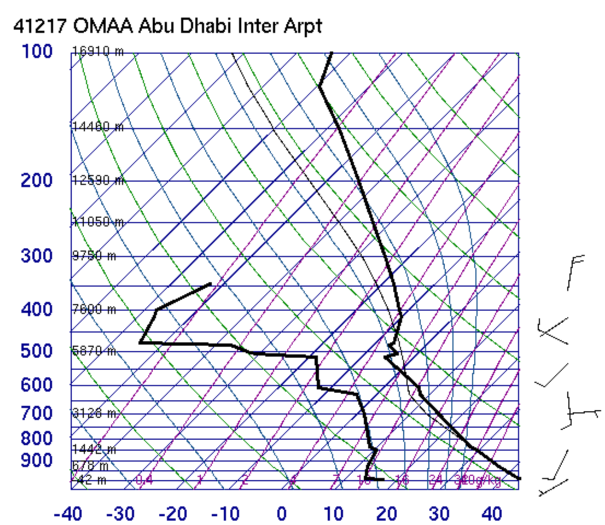

Figure 2. Abu Dhabi sounding (skewT-logP) at 12Z on 10 July 2004. Cloud base was at ~790 hPa.

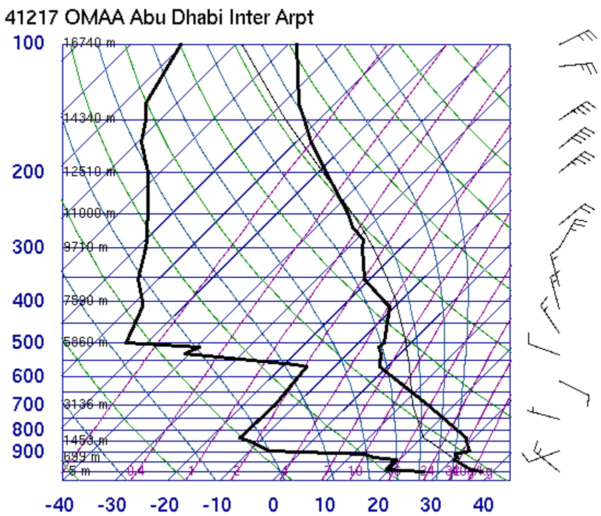

Figure 3. Abu Dhabi sounding (skewT-logP) at 12Z on 12 September 2004. Cloud base was at ~650 hPa.

On 10 July, low-level moisture causes a drastically different stability than on 12 September, yielding a low warm cloud base (~2.2 km and +23° C) and more vigorous and widespread convection. The upper level dryness and weak wind shear act to dissipate the storms that develop. On 12 September, the stable layer is not particularly strong, suggesting that convection has the potential of pushing through the 400 hPa level to perhaps as high as the 250 hPa level. However, the elevated cloud bases (~3.6 km and +10° C) and the extreme dryness above 550 hPa (~5 km and -2° C) also suggest that weaker convective pulses will have suppressed tops.

With such a difference in cloud base between the two days, the height of the first radar echo might be expected to show a similar difference. In particular, warmer bases might indicate a higher likelihood of a dominant warm rain process and therefore lower first echo heights. However, examination of several cells on each day (chosen to be the initial cells of the day or isolated from nearby cells) show echo height differences opposite to the cloud base differences. On 10 July, the first echo height ranges from 6.0 to 7.5 km MSL, while on 12 September the heights range from 4.5 to 5.25 MSL. (The radar resolution in the vertical is 0.75 km.) To further understand these differences, the radar echo development for a small variety of cells was examined. Figure 4 is a plot of the initial reflectivity growth rate versus cloud top growth. Although the two weakest cells (smallest growth rates) come from the 12 September sample, both days have cells that develop rapidly. There is an indication that initial reflectivity growth is related to cloud top growth, but it is a tenuous relationship that requires vastly more samples. So, while it is evident that convective overturning on 10 July is capable of lofting a substantial amount of precipitation mass, vigorous cells exist on 12 September that also loft precipitation, potentially affecting nearby cells.

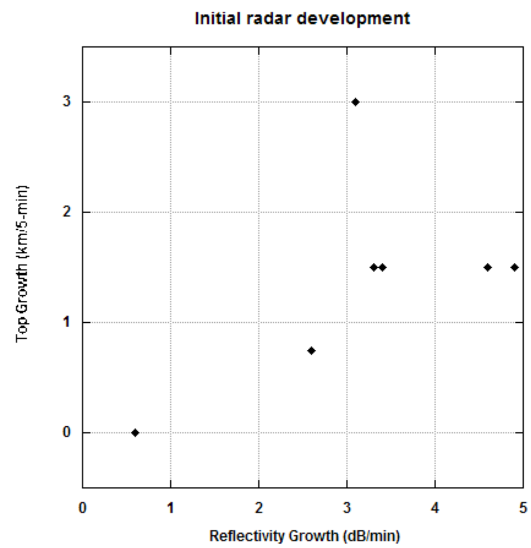

Figure 4. Reflectivity growth (dB/min) versus echo top growth (km/5-min) over the same initial 5-min time period for three widely spaced isolated cells on 10 July and four similarly chosen cells on 12 September. The 12 September sample includes the case study cell and an earlier cell near the eventual case study.

One example of a vigorous storm on 12 September is the first major storm in the operations area, which developed as part of a second cycle of storms about 70-80 km southeast of Al Ain. The height of the first echoes in the area (~0 dBZ at 10:45) was at 4.5-5.0 km, near the 0° C level. The storm was multi-cellular, and cells typically developed into sizes of 10-15 km. At 11:35 UTC, two main cells are dominant (Figure 5). The top is near its maximum of 11 km at this time although the large majority of the mass is below 6.5 km. A cross-section from northwest to southeast through the core of the cells is shown in Figure 6. The hint of a detrainment layer is evident at 4–6 km, particularly on the southeast (downwind) side of the northwest cell.

Photographic evidence from the research aircraft at 12:10 showed the storm tops to be dissipating. Remains of the southeast cell of Figure 5 were evident as a thin iced cloud, while the top of the northwest cell was beginning to detach. Also evident was an extensive cloudy region and detrainment layer at roughly the aircraft altitude of 5 km.

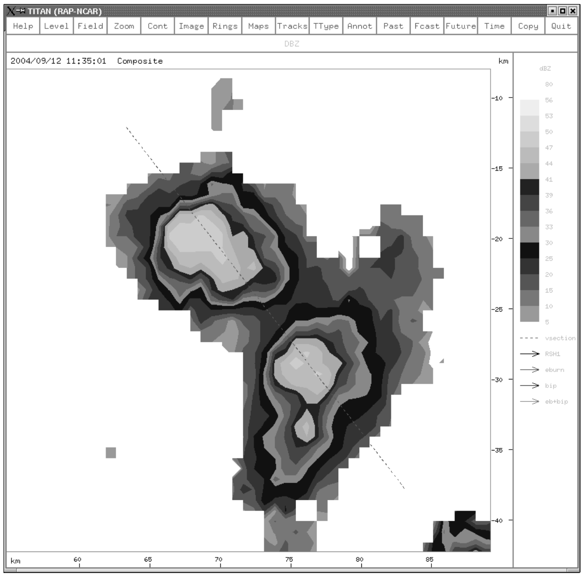

Figure 5. CAPPI of composite reflectivity (maximum dBZ at any level) at 11:35 UTC on 12 Sept 2004. Area is about 30 km x 30 km. Reflectivity scale increments by 5dB from 5 dBZ to 30 dBZ, then by 3 dB from 30 dBZ to 56 dBZ. The shading is shown at the right (e.g., maximum reflectivity in NW cell is 48 dBZ). The dashed line (from the northwest to the southeast) shows the location of the cross-section in Figure 6.

4. 12 SEPT 2004 – CASE STUDY STORM

4.1 Radar

After sampling cells near the previously mentioned storm, the research aircraft settled on a growing cloud mass 50 km east of Al Ain at 12:50. This storm lasted about 1 hr and initially appeared to be uni-cellular. In fact, three or four different updraft pulses and two moderate reflectivity cores occurred over this time period, reflecting the small-scale complexity of precipitation development under close examination. The top of this storm is considerably lower than that of the initial storm, and the bulk of the mass is below 6 km. Maximum reflectivities are several dB less as well.

The CAPPI in Figure 7 is near the time of the maximum echo top, and represents the reflectivity area at 5.25 km, near the height of the aircraft passes. The aircraft track for a 10-min period is also plotted in Figure 7 and shows that the aircraft passes, while below the visually most active tops, are slightly west of the echo core. The tightest reflectivity gradients can be seen along the west to north side of the cell. More particles appear to be spreading out in the southeast quadrant, which is the downwind side. A cross-section through the core at 13:35 (not shown) verifies that the maximum top was around 9 km with a substantial region of detrained reflectivity at 5-6 km – greatest on the south side.

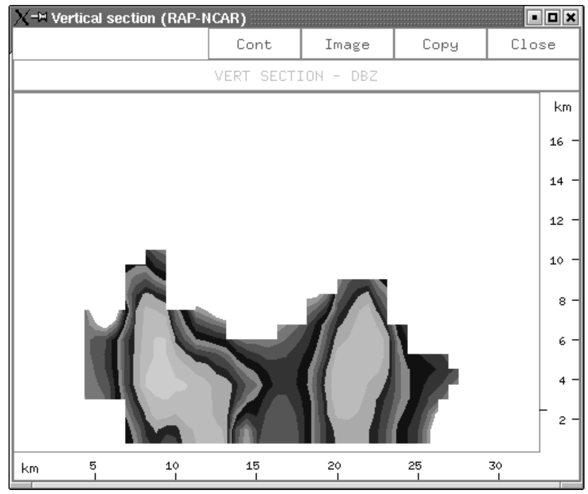

Figure 6. Cross-section of the reflectivity cells in Figure 5, NW (left) to SE (right). Reflectivity shading is the same as in Figure 5.

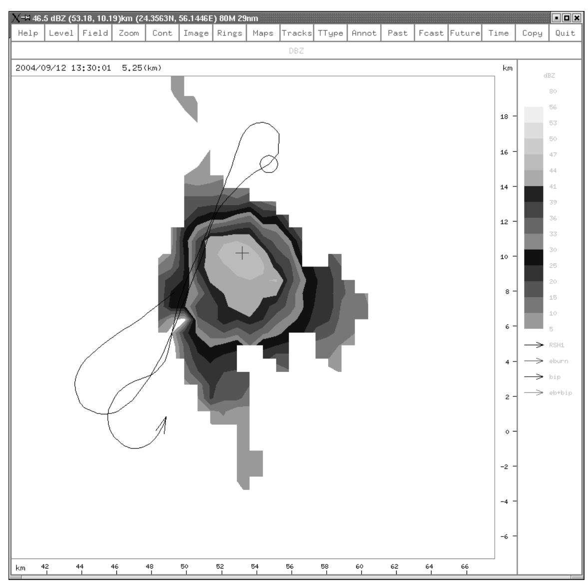

Figure 7. CAPPI of reflectivity at 5.25 km MSL and at 13:30 UTC on 12 Sept 2004. Area is about 25 km x 25 km. Black line shows the aircraft track from 13:25 to 13:35 (circle is at 13:30).

4.2 Aircraft

Seventeen storm penetrations were made over the course of about 70 min (12:51-13:59), the last four being in the precipitation shaft below cloud base. Time-series plots from the 13 cloud passes are shown in Figure 8. Penetrations were made around the -5° C level, although they were closer to -3° C after 13:25. Cloud droplet concentrations remained fairly consistent and high for most of the passes, even though they were about 2 km above cloud base. Few cloud particles existed before ~13:00, and significant precipitation particles were not detected until after ~13:15.

A short 5-min break from penetrations occurred after 13:08 to deal with wing icing from the first six cloud passes. At 13:01, the cloud base seeding aircraft began ‘treatment’, which turned out to be a no-seed case for this storm. The best updraft area at cloud base, at least during treatment from 13:01 to 13:16, was in the northwestern quadrant of the cell. Photographic evidence a short while later (13:23) confirmed that tops were growing to 8-9 km, and the cloud mass of the storm appeared to be made up of three or more turrets. A significant amount of cloud bulged outward at around 6 km (500-1000 m higher than the aircraft).

More detailed time-series plots from the cloud penetration passes shown in Figure 7 are given in Figure 9. The penetrations were made at 5.0-5.5 km, corresponding to -2 to -5° C with ~2° buoyant excursions in the updraft on the north side (around 13:28:45 and 13:32:00). Peak droplet concentrations remained quite constant at 650-750 cm^{-3} over the 10 passes up to this time, although the LWC dropped from peaks slightly greater than 2.0 g m^{-3} to 1.5 g m^{-3} or less. An interesting feature that developed on the north side, as shown in the two passes of Figure 9, is the existence of 2DC particles outside of the LWC region. To the aircraft observer, it appeared as though the particles were falling from thin to non-existent cloud. Similar particles and concentrations were sampled on the south side but within cloudy air (referred to in the observer’s notes as ‘debris’ cloud).

A sample of images from the 2DC at around 13:29 (Figure 10), just on the edge of the updraft and LWC region at the north side of cell in the first pass of Figures 7 and 9, demonstrates a wide range of particle types and sizes. At these temperatures and especially near and in the updraft, the size of the larger rimed graupel particles suggest either frozen drop embryos or potential recycling of earlier grown particles. There appear to be some drizzle-like images, along with several artifacts (which render the shadow-or counts unreliable for comparison with other passes). These larger particles also exist outside of the LWC region, possibly contributing to the recycling of particles in this and other cells. Further 2D analysis is required for better determination of the development of drizzle and the ice phase.

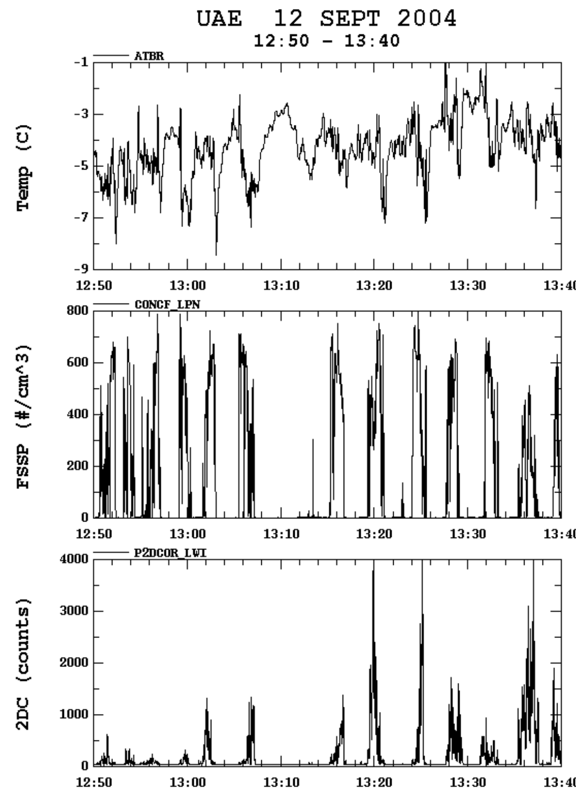

Figure 8. Time series plots on 12 Sept 2004 from 12:50 to 13:40 of thirteen penetrations through the case study storm. Top plot is temperature, middle plot is FSSP concentration, and bottom plot is 2DC shadow-or counts (unedited - includes artifacts).

5. SUMMARY

The storms that formed on 12 September 2004 and described here are fairly typical of storm conditions over the Oman Mountains in the summer. A ubiquitous subsidence inversion often suppresses convection. A weakening of the inversion, coupled with other factors such as low-level moisture or circulations creating convergence zones, leads to cycling of convective clouds and storms and often to the formation of precipitation. The radar data on 12 September show that earlier convection likely pre-conditioned the region with mid-level moisture and ice particles. Subsequent cells and storms developed significant precipitation as they grew above 6 km (around -5° C). This is consistent with the concept that recycling particles into the same and adjacent turrets is an important process in precipitation development. Other studies have shown similar results, both for primary ice initiation and development as well as for processes involving melted recycled particles (e.g., Dye *et al.,* 1983; Willis *et al.,* 1994). These studies and others have also documented the rapid development of precipitation (high reflectivity growth rates), which are often related to the mechanism of particle recycling.

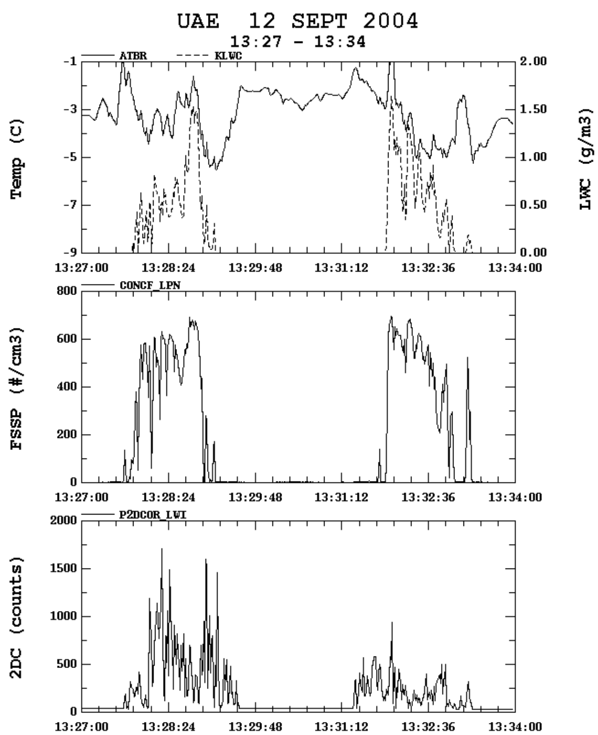

Figure 9. Time series plots on 12 Sept 2004 from 13:27 to 13:34 of two penetrations along the same path (as shown in Figure 7). Top plot is temperature (solid) with scale on the left and hot-wire liquid water content (dashed) with scale on the right. Middle plot is FSSP concentration and bottom plot is 2DC shadow-or counts (unedited – includes artifacts).

Since no seeding occurred in these storms, the question remains whether a seeding technique designed to increase drizzle formation would have helped the precipitation process in the 'second shift' storms, or helped to increase particles in the initial storms, or had no effect since the process might have already been efficient.

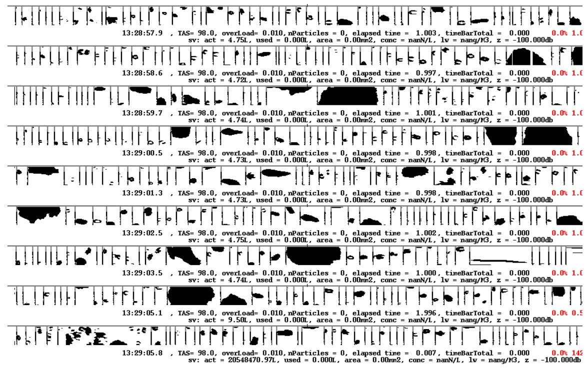

Figure 10. 2DC unedited images (13:28:58 to 13:29:06) on 12 Sept 2004.

More details from the other penetrations on this day and from cases on other days (both seeded and unseeded) should shed light on these possibilities. Certainly, the UAE studies re-emphasize the potential that detailed polarimetric radar information could have in delineating the precipitation process over a wide range of conditions and a large sample of storms.

Acknowledgements

This research was funded by the Department of Water Resources Studies of the Ministry of Presidential Affairs, United Arab Emirates. Special thanks go to Abdulla Al Mangoosh, Director, and Abdulla Al Mandoos, Head of Meteorology Section, for their support and encouragement. Thanks are due to all the field project participants, too numerous to mention, whose skill and hard work made the collection of these data so successful.

6. REFERENCES

Dixon, M.J., and G. Weiner, 1993: TITAN – Thunderstorm identification, tracking, analysis, and nowcasting – a radar-based methodology. *J. Atmos. Oceanic Tech.,* **10**, 785-797.

Dye, J.E., B.E. Martner, and L.J. Miller, 1983: Dynamical-microphysical evolution of a convective storm in a weakly-sheared environment. Part I: Microphysical observations and interpretation. *J. Atmos. Sci.,* **40**, 2083-2096.

Dye, J.E., W.P. Winn, J.J. Jones, and D.W. Breed, 1989: The electrification of New Mexico thunderstorms. 1. Relationship between precipitation development and the onset of electrification. *J. Geophys. Res.,* **94**, 8643-8656.

Huston, M.W., A.G. Detwiler, F.J. Kopp, and J.L. Stith, 1991: Observations and model simulations of transport and precipitation development in a seeded cumulus congestus cloud. *J. Appl. Meteor.,* **30**, 1389-1406.

Knight, C.A., W.D. Hall, and P.M. Roskowski, 1983: Visual cloud histories related to first radar echo formation in Northeast Colorado cumulus. *J. Appl. Meteor.,* **22**, 1022-1040.

Pakesh, P., 1998: Mechanisms of precipitation initiation in convective clouds around Delhi: A radar study. *Indian J. Radio and Space Physics,* **27**, 7-10.

Raymond, D.J., and A.M. Blyth, 1989: Precipitation development in a New Mexico thunderstorm. *Quart. J. Royal Meteor. Soc.,* **115**, 1397-1423.

Willis, P.T., J. Hallett, R.A. Black, and W. Hendricks, 1994: An aircraft study of rapid precipitation development and electrification in a growing convective cloud. *Atmos. Res.,* **33**, 1-24.